RSC Advances

PAPER

View Article Online
View Journal | View Issue

Cite this: *RSC Adv.*, 2022, **12**, 30704

Direct Michael addition/decarboxylation reaction catalyzed by a composite of copper ferrite nanoparticles immobilized on microcrystalline cellulose: an eco-friendly approach for constructing 3,4-dihydrocoumarin frameworks†

Bhupender Kumar, [a] Biplob Borah, [a] J. Nagendra Babu [b] and L. Raju Chowhan [*a]

A composite of copper ferrite oxide nanoparticles immobilized on microcrystalline cellulose ($CuFe_2O_4$@MCC) was synthesized. The synthesized composite was characterized by FESEM with EDS-Mapping, TEM, P-XRD, TEM, and BET analysis and investigated for its catalytic activity toward Tandem Michael addition and decarboxylation of coumarin-3-carboxylic acid with cyclic 1,3-diketones to obtain novel 3,4-dihydrocoumarin derivatives. This protocol was established with wide substrate scope and significant yield. The significant characteristics of this methodology are mild reaction conditions, easy setup procedure, non-toxic, and cost-effectiveness. A gram-scale synthesis with low catalyst loading was also demonstrated.

Received 22nd September 2022
Accepted 18th October 2022

DOI: 10.1039/d2ra05994k

rsc.li/rsc-advances

Introduction

In organic synthesis, the construction of active pharmaceutical ingredients containing heteroatoms has been considered a key domain for the development and design of drugs in medicinal and pharmaceutical chemistry, as well as in materials science.[1,2] Among diverse oxygen-heterocycles, coumarin (also known as the 2*H*-chromen-2-one ring) comprises a significant class of structural scaffolds in synthetic organic chemistry with the distinctive benzo-α-pyrone core in its fragment.[3] They are frequently found in the fundamental structure of many natural products and synthetic compounds and have been recognized in a large number of pharmaceutically useful components and drug candidates.[4] Ningalin B (**A**), a marine natural product with coumarin at its core, has been known to have immunomodulatory and HIV-1 integrase inhibitory properties.[5,6] The natural product (+)-calanolide A (**B**) isolated from *Calophyllum lanigerum* was discovered to exhibit anti-HIV activity[7–9] whereas (+)-cordatolide A (**C**) is the key inhibitor of HIV-reverse transcriptase.[10] Warfarin (**D**), another natural product derived from woodruff and lavender with 4-hydroxycoumarin as its key component was used to reduce the blood clotting in the veins, heart, or lungs, (Fig. 1).

Aside from natural compounds and their analogs, synthetic coumarin derivatives have become significantly more appealing in recent years for their impressive biological and pharmacological activities, such as antimicrobial,[11] antioxidant,[12] analgesic,[13] anticancer,[14–16] and antituberculosis[17] properties. The significant potentiality of coumarin and its derivatives in material sciences includes solar energy, laser dyes, optical recording, oxygen sensors, nonlinear optical chromophores,

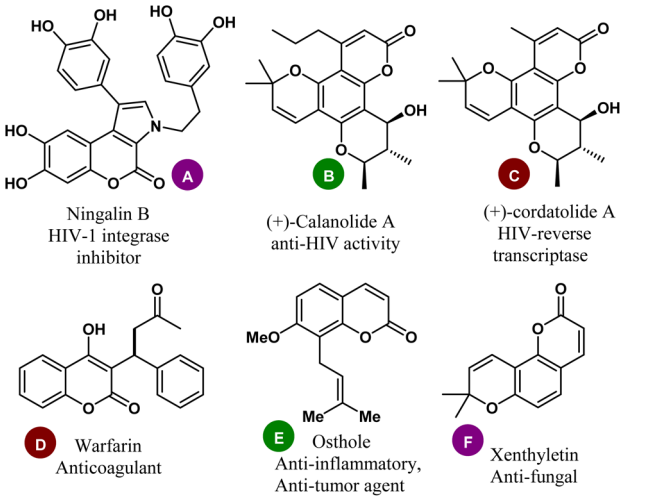

Fig. 1 Representative examples of coumarin-based natural products with relevant therapeutic significance.

[a]*School of Applied Material Sciences, Central University of Gujarat, Sector 30, Gandhinagar, Gujarat 382021, India. E-mail: rajuchowhan@gmail.com; rchowhan@cug.ac.in*

[b]*Department of Chemical Sciences, School for Basic and Applied Sciences, Central University of Punjab, Ghudda, Bathinda, 151401, India*

† Electronic supplementary information (ESI) available. See DOI: https://doi.org/10.1039/d2ra05994k

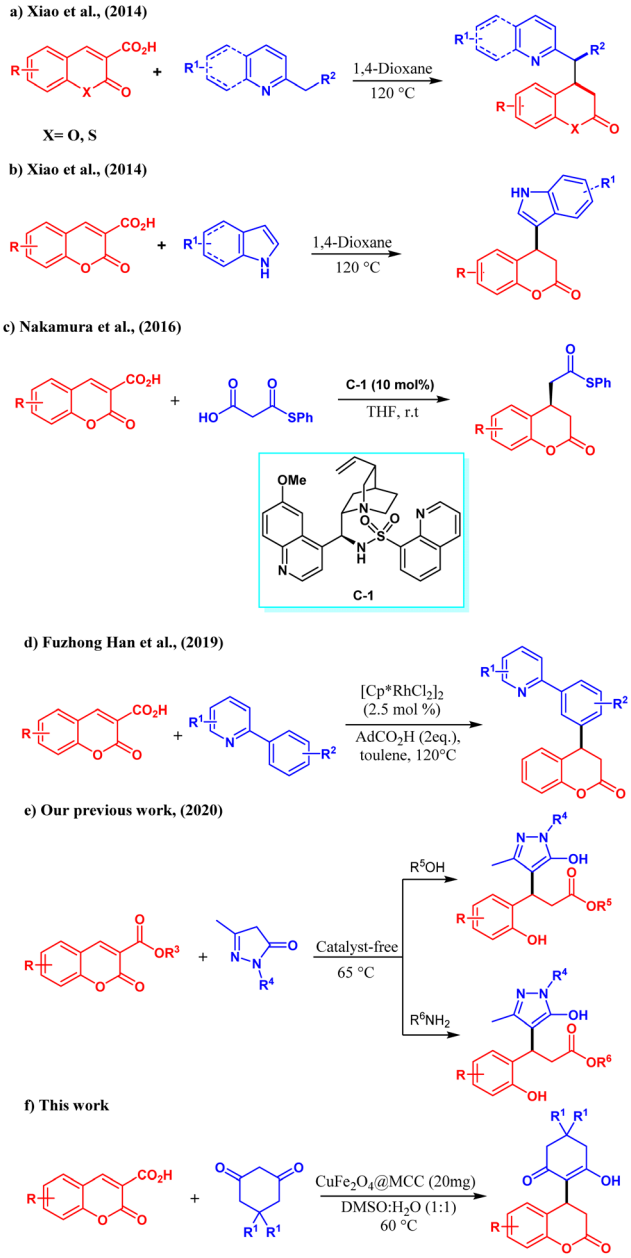

Scheme 1 Synthesis of 3,4-dihydrocoumarins.

molecular photonic devices, polymers, optical brighteners, and fluorescent probes, chemosensors, whiteners has also been well explored.[18–21] Additionally, fluorescent nanoparticles like graphene and carbon quantum dots, which have found extensive use in biological imaging experiments, were synthesized by employing coumarin and its derivatives.[22,23] Considering the tremendous therapeutic significance and broad-spectrum chemical landscape of coumarins, the past decades have witnessed immense efforts not just for their synthesis but also Scheme 1 for their utilization as a testing ground in the discovery of new reactions and the synthesis of complex hybrid molecules of medicinal interest.[24]

Especially, the exploitation of carboxylic acid/ester functionalized coumarins as Michael acceptors for the assembly of 3,4-dihydrocoumarin has recently gained immense importance. But, due to loosing its aromatic nature, harsh reaction conditions are desired which marks the limitations of the reaction scopes as previously reported works, Michael addition *via* ring-opening/decarboxylation at high temperature or using organocatalyst.[25] In 2014 Xiao *et* al. reported a lot of work on coumarin, Michael addition followed by decarboxylation of coumarin-3-carboxylic acid with without any catalyst aza arenes for the synthesis of functionalized 3,4-dihydrocoumarin.[26] They also disclosed the exploitation of indoles as the nucleophiles for the direct Michael addition with coumarin-3-carboxylic which is followed by decarboxylation to form diverse 3,4-dihydrocoumarin derivatives.[27] In 2016 Nakamura *et* al. described the asymmetric synthesis of functionalized 3,4-dihydrocoumarin using malonic acid half-thioesters and coumarin-3-carboxylic acid in the presence of cinchona derived chiral organocatalyst **C-1**.[25] In 2019 Hu, Han, and co-workers devised Rh(III)-catalyzed a traceless C–H activation strategy for the synthesis of 3,4-hydroxycoumarins by a conjugate addition/decarboxylations of coumarin-3-carboxylic acid and 2-aryl pyridines.[28] Encouraged by these promising results, our group also tested the reactivity of carboxylic acid/ester functionalized coumarin towards the reaction with pyrazolones at 60 °C. Changing the solvent system to either water/alcohol or amines in catalyst-free conditions followed tandem conjugate addition/decarboxylation and esterification/amidations to form different pyrazole derivatives.[24] Given above most of the previously reported reaction on coumarins leads to ring opening and very few reactions retains in the core structure. On the other hand, in the last decade for the C–C bond formation metal oxide nanoparticles were used in place of the organic base for controlling ring-opening, and side products as well as occurring the addition at normal temperature. Metallic and bimetallic nanoparticles are the most interesting catalysts for C–C bond formation due to having robust qualities especially such as a higher surface area with stability and easy separation.[29] These qualities make them appropriate for various applications with a wide range of catalysis.[30]

However, during the application of metal oxide nanoparticles, some drawbacks are faced like leaching and recovery. In the case of magnetic nanoparticles, agglomeration was observed as a major drawback. To restrain these drawbacks, stabilizers and immobilizers are used to provide a surface.[31] Recently, we synthesized Cu_2O@MCC and Fe_3O_4@MCC and studied their catalytic activity towards 1, 3-dipole cycloaddition and Michael addition. The catalytic activity of Cu_2O@MCC was studied for the 1,3 dipolar cycloaddition of chalcone/styrylisoxazoles on azomethine ylide of isatin and THIQ.[32] Fe_3O_4@MCC and Fe_2O_3@MCC were studied for Michael addition of 1,3 diketones on styrylisoxazoles and 1,3-dipole reaction of acetyl oxime/azirine with alkyne respectively.[2,33] MCC is used to improve the stability and reactivity of nanoparticles by providing a surface. Due to the distinctive morphology, renewability, lightweight, and nanoscale dimension of MCC, it emerged as an important material for the strengthening of nanocomposite.[34–36]

In the present work, we synthesized $CuFe_2O_4$@MCC and characterized it by FESEM with EDS-Mapping, TEM, P-XRD, TEM, and BET analysis. The synthesized composite has been studied for the reactivity of cyclic 1,3-diketones on coumarin-3-carboxylic acid to obtain novel 3,4-dihydrocoumarins. The obtained products were characterized by IR, NMR, and LCMS. Consequently, for the first time, we report here a direct Michael addition, as well as decarboxylation of coumarin-3-carboxylic acids, and devised the reactivity of cyclic 1,3-diketones.

Results and discussion

Synthesis and characterization of copper ferrite nanoparticles ($CuFe_2O_4$) immobilized on microcrystalline cellulose composite

Synthesis of 30% (w/w%) loading of copper ferrite nanoparticles on microcrystalline cellulose nanocomposites was done by using the precipitation technique. In a 500 mL beaker, 1.184 g of copper sulphate pentahydrate and 1.728 g of ferric chloride in 100 mL water were taken and heated at 90 °C with stirring at 600 rpm. After obtaining a homogenous mixture, 2.1 g of microcrystalline cellulose was added to the reaction mixture. For the synthesis of the copper ferrite nanoparticles, an aqueous solution of 2 N NaOH was added at 90 °C. To obtain homogeneity of the composite, addition of aqueous NaOH was done at the rate of 2 mL per minute. The black material was separated and washed with deionized water and methanol. The material was vacuum dried to obtain the famish $CuFe_2O_4$@MCC.

Field emission scanning electron microscope (FESEM) analysis was done to confirm the binding of $CuFe_2O_4$ on MCC. From the FESEM image, we observed heterogenous immobilization of $CuFe_2O_4$ on MCC (Fig. 2a). Energy-dispersive X-ray spectroscopy (EDS) spectrum (Fig. 2b) of composite confirms the presence of copper (Cu), carbon(C), iron (Fe), and oxygen (O).

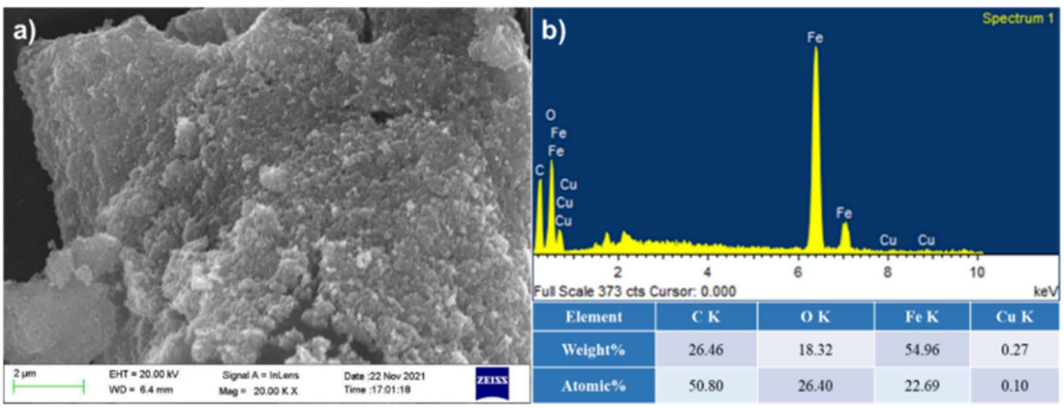

Element	C K	O K	Fe K	Cu K
Weight%	26.46	18.32	54.96	0.27
Atomic%	50.80	26.40	22.69	0.10

Fig. 2 (a) SEM image (b) EDS analysis of $CuFe_2O_4$@MCC.

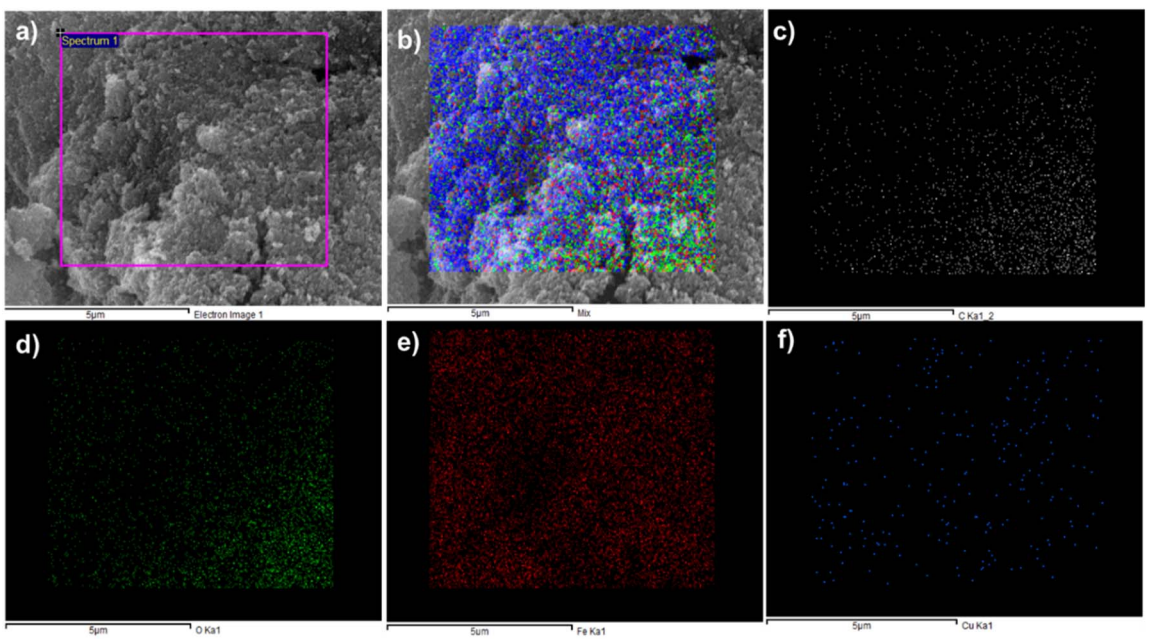

Fig. 3 Elemental mapping of $CuFe_2O_4$@MCC (a) electron image (b) mix (c) carbon (d) oxygen (e) iron and (f) copper.

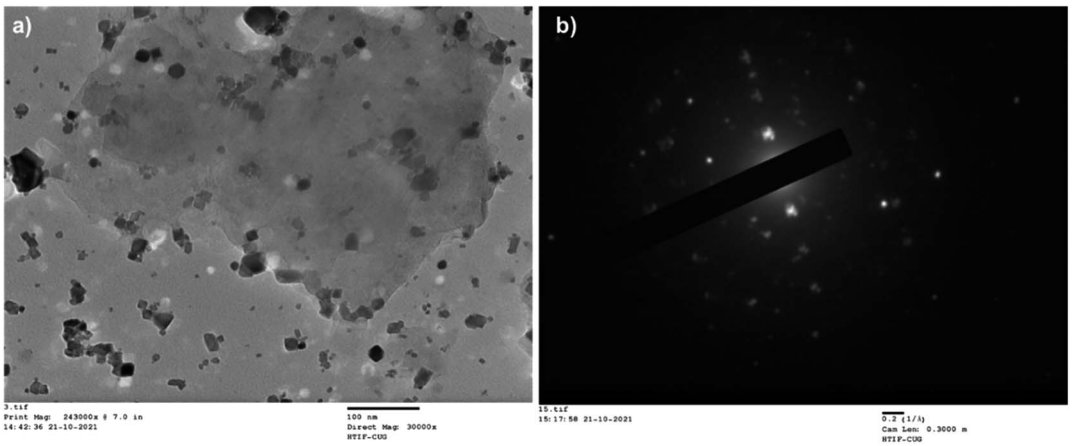

Fig. 4 (a) TEM image and (b) SAED pattern of $CuFe_2O_4$@MCC.

Elemental Mapping of the composite has also sported the presence of carbon and oxygen with both metal iron and copper. As shown in Fig. 3a electron image (**3b**), mix mapping of composite having all elements of composite, and (**3c**) and (**3d**) are for the carbon and oxygen. In Fig. 3(e) and (f) presence of iron and copper was observed.

Transmission Electron Microscope (TEM) analysis was done to confirm the immobilization as well as the particle size of $CuFe_2O_4$ and the nature of the composite (Fig. 4(a)and (b)).

The size of $CuFe_2O_4$ nanoparticles was observed less than 50 nm and immobilized on MCC. From SAED pattern confirms the polycrystalline nature of synthesized composite. For the confirmation of $CuFe_2O_4$, powder X-ray diffraction was done (Fig. 5a). An X-ray diffraction pattern of $CuFe_2O_4$@MCC composite gave sharp reflections at $2\theta = 15.82°$, and 22.79° for crystalline cellulose with $2\theta = 18.51°$, 30.64, 35.74°, 43.35°, 53.66, 57.35°, 57.35°, and 62.92 having plane (111), (220), (311), (400), (422), (511), and (440), respectively, which confirms the construction of $CuFe_2O_4$ nanoparticles.[37] From previous literature, we also confirm that the synthesized composite doesn't contain any iron oxide (Fe_3O_4, Fe_2O_3) and copper oxide (Cu_2O, CuO) nanoparticles.[2,32,33,38,39] Thermogravimetric analysis (TGA) under an inert condition at room temperature to 600 °C with a constant heating rate of 10 °C per minute was done for studying the thermal stability of $CuFe_2O_4$@MCC composite (Fig. 5b). 8% degradation was observed from room temperature to 120 °C due to the loss of hydroxy groups and water from cellulose. Another 6% loss of weight was observed up to 277 °C and a sharp degradation of 38% was observed in the temperature range 277 to 375 °C, which carries degradation of microcrystalline cellulose from composite. Therefore, a total of 52 and 65% degradation was observed from 375 to 600 °C respectively. TGA analysis confirms composite is more thermally stable than MCC. Catalysis is a surface phenomenon therefore Brunauer–Emmett–Teller (BET) analysis was done to examine the surface area of the composite $CuFe_2O_4$@MCC under inert conditions. The significant results was found with average pore diameter of 28.186 nm and 15.77 $m^2\ g^{-1}$ surface area. The surface area of the composite is 12.13 times higher than MCC.[35]

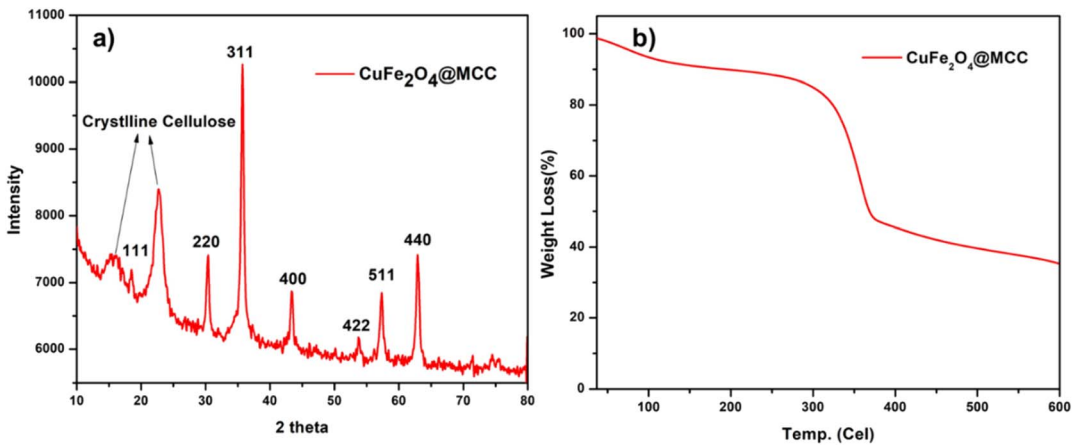

Fig. 5 (a) Powder X-ray diffraction and (b) TGA analysis of $CuFe_2O_4$@MCC.

Table 1 Optimization of $CuFe_2O_4$@MCC catalyzed Michael addition of 5,5-dimethyl-cyclohexane-1,3-dione on coumarin 3-carboxylic acid[a]

Entry	Solvent	Catalyst loading	Temp. (°C)	Time	Yield[b] (%)
1	H_2O	—	RT	48 h	—
2	H_2O	10 mg	RT	48 h	—
3	H_2O	20 mg	RT	48 h	—
4	H_2O	10 mg	50	12 h	22
5	H_2O	15 mg	50	12 h	48
6	H_2O	20 mg	50	12 h	56
7	H_2O	20 mg	60	12 h	61
8	H_2O	25 mg	60	12 h	62
9	EtOH/H_2O 1 : 2	20 mg	60	7 h	65
10	EtOH/H_2O 1 : 1	20 mg	60	7 h	69
11	DMSO/H_2O 1 : 4	20 mg	60	7 h	68
12	DMSO/H_2O 1 : 2	20 mg	60	7 h	78
13	DMSO/H_2O 1 : 1	20 mg	60	7 h	86

[a] Reaction condition: the reaction was conducted using 1 mmol of 5,5-dimethyl-cyclohexane-1,3-dione **1a** and 1 mmol of coumarin 3-carboxylic **2a**, in 3 mL of solvent with stirring at various temperatures for different times as indicated. [b] Isolated yield.

The composite of $CuFe_2O_4$ nanoparticles immobilized on MCC was used as a catalyst, and catalytic activity was studied for Michael addition of 5,5-dimethyl-cyclohexane-1,3-dione **1a** on coumarin 3-carboxylic **2a**. Initially, the reaction was studied without catalyst, with 10 mg and 20 mg of $CuFe_2O_4$@MCC in the water at room temperature, for 48 hours and did not observe the change in reactants (Table 1 entries 1–3). The reaction was done in presence of 10 mg of $CuFe_2O_4$@MCC and stirred at 50 °C for 12 h to obtain the Michael adduct **3a** having 22% yield (Table 1, entry 4). On increase the loading of $CuFe_2O_4$@MCC to 15 mg and 20 mg, the significant increase was observed in yield, up to 48 and 56% respectively (Table 1, entries 5 and 6). The reaction temperature increased to 60 °C and a slightly increased in yield was observed (61%). Loading of the composite was increased to 25 mg at a similar reaction condition and didn't get a significant increase in yield (Table 1, entry 8). The optimized reaction condition found that 20 mg of $CuFe_2O_4$@MCC composite gives a significant yield at 60 °C for 12 hours in an aqueous medium (Table 1, entry 7). Maintaining the green characteristics of the reaction and reducing the use of organic solvents make easy workup of reaction mixture and separation of the product. As we obtain significant results in our previous reports, the reaction was performed in an aqueous ethanolic solution. In the presence of 20 mg $CuFe_2O_4$@MCC composite in EtOH : H_2O (1 : 2) as solvent 65% yield was obtained (Table 1, entry 9), and in the case of EtOH : H_2O (1 : 1) slightly increase in yield was found up to 69% (Table 1, entry 10). Coumarin 3-carboxylic acids are soluble in DMSO, hence, to enhance the reactivity of $CuFe_2O_4$@MCC composite and yield of the analytical product we studied that reaction in aqueous dimethyl sulfoxide solution of different concentrations such as 1 : 4, 1 : 2, and 1 : 1 of DMSO : H_2O (Table 1, entries 11,12, and 13). We observed an 86% significant yield in 1 : 1 of DMSO : H_2O at 60 °C for 7 hours in presence of 20 mg of $CuFe_2O_4$@MCC composite (Table 1, entry 13). An optimized condition (Table 1, entry 13) was used to delve into substrate scope and found to assist the array of substrates, (Scheme 3, Table 2).

The reaction of dimedone/cyclohexane-1,3-dione (**1a**/**1b**) with halo substituted coumarin 3-carboxylic acid such 6-fluoro/chloro/6,8-dichloro/bromo-2-oxo-2*H*-chromene-3-carboxylic acid

Table 2 Substrate scope[a]

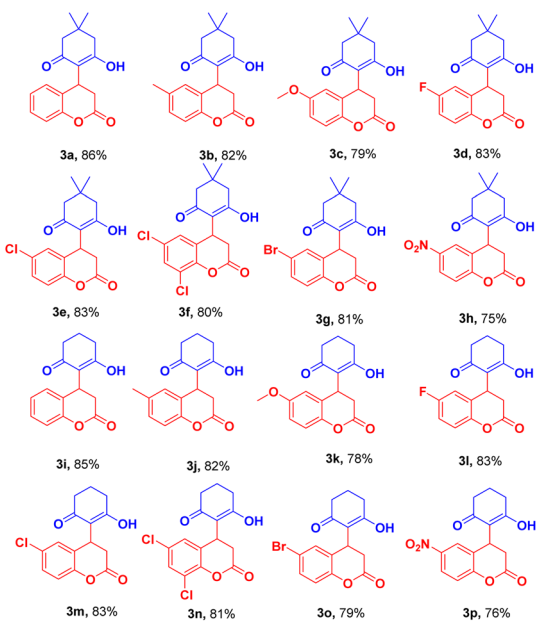

[a] Reaction condition: The reaction was conducted with 1.0 mmol of 5,5-dimethyl-cyclohexane-1,3-dione/cyclohexane-1,3-dione (**1a–b**), 1.0 mmol of coumarin 3-carboxylic acid (**2a–h**), and $CuFe_2O_4$ (20 mg) in aqueous DMSO in 1 : 1 (3 mL). Yields of the isolated product (**3a–o**). Reaction time: 7 h.

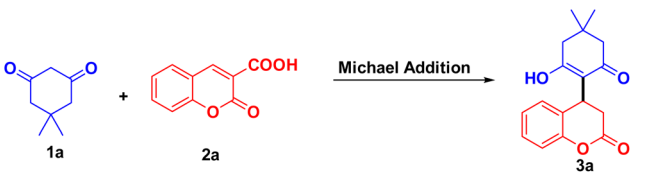

Scheme 2 Optimization of reaction condition.

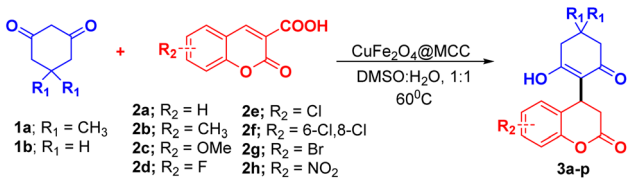

Scheme 3 Substrate scope.

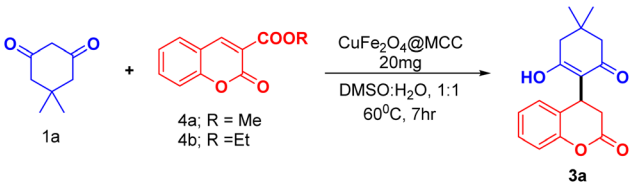

Scheme 4 Extension of the work towards coumarin 3-carboxylic esters.

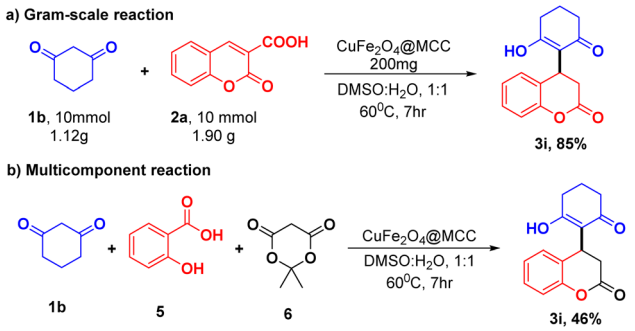

Scheme 5 (a) Scaleup reaction and (b) multicomponent reaction.

afforded the product in excellent yield (Table 2, **3d–g, 3l–o**). In the case of nitro substituted coumarin 3-carboxylic acid with **1a/b** slightly lower analytical product was observed (Table 2, **3h, 3p**).

We exploit the reaction of dimedone **1a** with coumarin 3-carboxylic ester (**4a, 4b**) under optimized conditions (Table 1, entry 13). We observed the same product (**3a**) (Scheme 4) with approximate yield as observed in case of coumarin 3-carboxylic acid. In the case of Scheme 2, the reaction was found to be preceded by decarboxylation whereas coumarin 3-carboxylic **4a/b** proceeds by ester hydrolysis followed by decarboxylation.

Scaleup and multicomponent experiment

A gram-scale reaction was set up on a 10 mmol scale to validate the applicable protocol. Synthesis of **3a** was investigated to find the ability of the established protocol. Appropriately, 10 mmol of **1b** and **2a** were treated using optimized reaction conditions (Table 1, entry 13) and obtained significant product **3i** in 85% yield. In addition to that protocol, the optimized reaction conditions (Table 1, entry 3) were also exploited to perform a multicomponent reaction of 1,3 cyclohexanedione (**1b**), salicylaldehyde (**5**), and meldrum acid (**6**) with $CuFe_2O_4$@MCC composite a one-pot approach. Surprisingly, in the optimized condition, we observed the desired product (**3i**) with a 46% yield (Scheme 5) and on increasing reaction time 12 h, no significant increase in yield was observed.

Conclusions

In this report, we study the catalytic activity of $CuFe_2O_4$@MCC composite toward Michael Addition of 5,5-dimethyl-cyclohexane-1,3-dione/cyclohexane-1,3-dione and 3-carboxylic coumarins for the synthesis of 3,4-hydroxycoumarins. Synthesis, characterization, and reactivity of composite having two widely available metals with bio-degradable polymer are studied. The catalytic property of $CuFe_2O_4$@MCC investigated for nucleophilic addition of 1,3 cyclic diketones on coumarin-3-carboxylic acid in presence of 1 : 1 solvent systems of H_2O : DMSO. The products were isolated without any purification techniques such as column chromatography with 75–86% yield. Synthesized composite has shown excellent catalytic activity for the construction of 3,4-Dihydrocoumarin frameworks and a comparison study of previously reported methods are shown in Scheme 6.[40–44] Due to easy separation of composite as well as significant product, simple and safe process for reaction setup, and moderate reaction time, this protocol also provides the potential as alternative applicability in gram-scale synthesis.

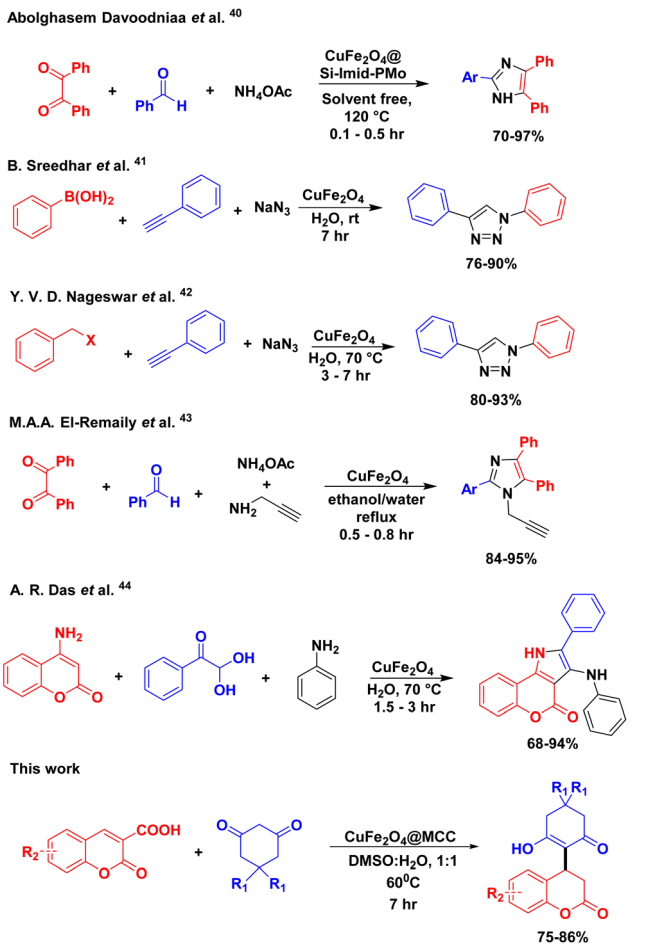

Scheme 6 Comparison of previously reported methods with the current method.

Author contributions

Bhupender Kumar; conceptualization-equal, data curation-equal, formal analysis-equal, investigation-equal, writing – original draft-equal Biplob Borah; writing – draft J. Nagendra Babu data curation-equal L. Raju Chowhan; supervision-equal.

Conflicts of interest

There are no conflicts to declare.

Acknowledgements

BK and BB gratefully acknowledge UGC for a Non-NET fellowship. The authors thank Central Instrumentation Facility of Central University of Gujarat and Central Instrumentation Laboratory, Central University of Punjab for various analyses.

Notes and references

1 B. Borah, K. D. Dwivedi, B. Kumar and L. R. Chowhan, *Arabian J. Chem.*, 2022, **15**, 103654.
2 K. D. Dwivedi, B. Kumar, M. S. Reddy, B. Borah, J. Nagendra Babu and L. R. Chowhan, *Results Chem.*, 2021, **3**, 100201.
3 C. Gleye, G. Lewin, A. Laurens, J.-C. Jullian, P. Loiseau, C. Bories and R. Hocquemiller, *J. Nat. Prod.*, 2003, **66**, 690–692.
4 K. P. Barot, S. V Jain, L. Kremer, S. Singh and M. D. Ghate, *Med. Chem. Res.*, 2015, **24**, 2771–2798.
5 H. Fan, J. Peng, M. T. Hamann and J.-F. Hu, *Chem. Rev.*, 2007, **108**, 264–287.
6 C. P. Ridley, M. V. R. Reddy, G. Rocha, F. D. Bushman and D. J. Faulkner, *Bioorg. Med. Chem.*, 2002, **10**, 3285–3290.
7 T. Ma, Q. Gao, Z. Chen, L. Wang and G. Liu, *Bioorg. Med. Chem. Lett.*, 2008, **18**, 1079–1083.
8 T. C. McKee, R. W. Fuller, C. D. Covington, J. H. Cardellina, R. J. Gulakowski, B. L. Krepps, J. B. McMahon and M. R. Boyd, *J. Nat. Prod.*, 1996, **59**, 754–758.
9 M. T. Flavin, J. D. Rizzo, A. Khilevich, A. Kucherenko, A. K. Sheinkman, V. Vilaychack, L. Lin, W. Chen, E. M. Greenwood, T. Pengsuparp, J. M. Pezzuto, S. H. Hughes, T. M. Flavin, M. Cibulski, W. A. Boulanger, R. L. Shone and Z.-Q. Xu, *J. Med. Chem.*, 1996, **39**, 1303–1313.
10 H. Ranjith, W. Dharmaratne, S. Sotheeswaran, S. Balasubramaniam and E. S. Waight, *Phytochem*, 1985, **24**, 1553–1556.
11 A. A. Zaha and A. Hazem, *New Microbiol.*, 2002, **25**, 213–222.
12 C. Kontogiorgis and D. Hadjipavlou-Litina, *J. Enzyme Inhib. Med. Chem.*, 2003, **18**, 63–69.
13 S. Khode, V. Maddi, P. Aragade, M. Palkar, P. K. Ronad, S. Mamledesai, A. H. M. Thippeswamy and D. Satyanarayana, *Eur. J. Med. Chem.*, 2009, **44**, 1682–1688.
14 C.-J. Wang, Y.-J. Hsieh, C.-Y. Chu, Y.-L. Lin and T.-H. Tseng, *Cancer Lett.*, 2002, **183**, 163–168.
15 M. Kaur, S. Kohli, S. Sandhu, Y. Bansal and G. Bansal, *Anticancer Agents Med. Chem.*, 2015, **15**, 1032–1048.
16 A. Thakur, R. Singla and V. Jaitak, *Eur. J. Med. Chem.*, 2015, **101**, 476–495.
17 R. S. Keri, S. B. Sasidhar, B. M. Nagaraja and M. A. Santos, *Eur. J. Med. Chem.*, 2015, **100**, 257–269.
18 X. Sun, T. Liu, J. Sun and X. Wang, *RSC Adv.*, 2020, **10**, 10826–10847.
19 S. R. Trenor, A. R. Shultz, B. J. Love and T. E. Long, *Chem. Rev.*, 2004, **104**, 3059–3078.
20 V. F. Traven, A. V Manaev, A. Y. Bochkov, T. A. Chibisova and I. V Ivanov, *Russ. Chem. Bull.*, 2012, **61**, 1342–1362.
21 D. Cao, Z. Liu, P. Verwilst, S. Koo, P. Jangjili, J. S. Kim and W. Lin, *Chem. Rev.*, 2019, **119**, 10403–10519.
22 Ł. Janus, J. Radwan-Pragłowska, M. Piątkowski and D. Bogdał, *Int. J. Mol. Sci.*, 2020, **21**(21), 8073.
23 Z. Yu, W. Ma, T. Wu, J. Wen, Y. Zhang, L. Wang, Y. He, H. Chu and M. Hu, *ACS Omega*, 2020, **5**, 7369–7378.
24 S. R. Lakshmi, V. Singh and L. R. Chowhan, *RSC Adv.*, 2020, **10**, 13866–13871.
25 S. Nakamura, A. Toda, M. Sano, T. Hatanaka and Y. Funahashi, *Adv. Synth. Catal.*, 2016, **358**, 1029–1034.
26 L. Xu, Z. Shao, L. Wang and J. Xiao, *Org. Lett.*, 2014, **16**, 796–799.
27 Z. Shao, L. Xu, L. Wang, H. Wei and J. Xiao, *Org. Biomol. Chem.*, 2014, **12**, 2185–2188.
28 F. Han, S. Xun, L. Jia, Y. Zhang, L. Zou and X. Hu, *Org. Lett.*, 2019, **21**, 5907–5911.
29 F. Scalambra, P. Lorenzo-Luis, I. de los Rios and A. Romerosa, *Coord. Chem. Rev.*, 2021, **443**, 213997.
30 D. Pla and M. Gómez, *ACS Catal.*, 2016, **6**, 3537–3552.
31 (*a*) S. Sarkar, E. Guibal, F. Quignard and A. K. SenGupta, *J. Nanopart. Res.*, 2012, **14**, 715–738; (*b*) K. D. Dwivedi, S. R. Marri, S. K. Nandigama and R. L. Chowhan, *J. Chem. Sci.*, 2018, **130**, 129.
32 B. Kumar, J. N. Babu and R. L. Chowhan, *Appl. Organomet. Chem.*, 2022, 1–14.
33 B. Kumar, M. S. Reddy, K. D. Dwivedi, A. Dahiya, J. N. Babu and R. L. Chowhan, *Appl. Organomet. Chem.*, 2021, 1–10.
34 O. A. Battista and P. A. Smith, *Ind. Eng. Chem.*, 2002, **54**, 20–29.
35 S. Ardizzone, F. S. Dioguardi, T. Mussini, P. R. Mussini, S. Rondinini, B. Vercelli and A. Vertova, *Cellulose*, 1999, **6**, 57–69.
36 E. C. Ramires, J. D. Megiatto, A. Dufresne and E. Frollini, *Fibers*, 2020, **8**, 21, DOI: **10.3390/fib8040021**.
37 M. Amir, H. Gungunes, Y. Slimani, N. Tashkandi, H. S. El Sayed, F. Aldakheel, M. Sertkol, H. Sozeri, A. Manikandan, I. Ercan and A. Baykal, *J. Supercond. Novel Magn.*, 2019, **32**, 557–564.
38 M. Amini, A. Pourvahabi Anbari, S. Ramezani, S. Gautam and K. Hwa Chae, *ChemistrySelect*, 2016, **1**, 4607–4612.
39 M. K. Satheeshkumar, E. Ranjith Kumar, C. Srinivas, G. Prasad, S. S. Meena, I. Pradeep, N. Suriyanarayanan and D. L. Sastry, *J. Magn. Magn. Mater.*, 2019, **484**, 120–125.
40 E. Teymoori, A. Davoodnia, A. Khojastehnezhad and N. Hosseininasab, *Q. J. Iran. Chem. Commun.*, 2019, **7**, 174–185.

41 A. S. Kumar, M. A. Reddy, M. Knorn, O. Reiser and B. Sreedhar, *Eur. J. Org. Chem.*, 2013, 4674–4680.
42 B. S. P. Anil Kumar, K. Harsha Vardhan Reddy, B. Madhav, K. Ramesh and Y. V. D. Nageswar, *Tetrahedron Lett.*, 2012, **53**, 4595–4599.
43 M. A. E. A. A. A. El-Remaily and A. M. Abu-Dief, *Tetrahedron*, 2015, **71**, 2579–2584.
44 M. Saha, K. Pradhan and A. R. Das, *RSC Adv.*, 2016, **6**, 55033–55038.